

# A Novel System Identification-Based Method for Rebar Radius Estimation in Radar SAR-Based Non-Destructive Testing

Kwang-Yeun Park, Joo-Hyung Lee, Changbin Joh

KOREA INSTITUTE of CIVIL ENGINEERING and BUILDING TECHNOLOGY, Korea, Republic of (South Korea)  
email: kypark@kict.re.kr, leejoohyung@kict.re.kr, cjoh@kict.re.kr

**ABSTRACT:** Non-destructive testing of reinforced concrete commonly utilizes electromagnetic waves, such as radar, to obtain internal structural information. When probing around rebars using electromagnetic equipment, hyperbolic-shaped images are often generated. Typically, image focusing techniques, including Hyperbolic Summation, Kirchoff Migration, Phase-shift Migration, Omega-k Migration, and Back-projection-based Focusing, which are based on Synthetic Aperture Radar (SAR) algorithms, are applied to analyze these hyperbolic images. However, these conventional methods cannot accurately determine the size of rebars and face limitations when inspecting doubly reinforced concrete due to shadow regions created by surface-layer rebars, which obscure the internal rebars. To address these challenges, this study proposes a novel approach that analyzes hyperbolic images based not on the image itself, but on the information related to wave propagation distances. In this method, the rebar cross-section is assumed to be a circle with an arbitrary radius, and a hyperbolic equation is established accordingly. The radius is determined by solving the equation using a system identification (SI)-based approach that minimizes the error between the measured hyperbola and the theoretical one. As with many conventional SI techniques, this problem is highly ill-posed, requiring the introduction of regularization methods to stabilize the solution.

**KEY WORDS:** System Identification (SI), Rebar Radius Estimation, Non-Destructive Testing (NDT), Radar SAR Imaging, Regularization Techniques.

## 1 INTRODUCTION

When non-destructive testing is performed on reinforced concrete using radar equipment, the result appears in a hyperbola as shown in Figure 1. Such hyperbola images can be processed using methods such as hyperbolic summation, Kirchoff migration, phase-shift migration, Omega-k migration, or back-projection-based focusing [1-5], or analyzed empirically to determine the position and size of the rebar. These methods are very useful for identifying the overall internal structure of concrete. They make it possible to detect the presence of materials other than concrete (e.g., rebar or voids) inside the concrete and to estimate their approximate size. However, only a relative size can be inferred; the exact size of the object remains unknown. While it is fairly easy to detect a missing rebar—omitted either by mistake or wrongdoing during construction—it is difficult to confirm whether a rebar with a smaller cross-sectional area than required was used. It is also challenging to verify significant reductions in effective cross-sectional area due to severe corrosion. Moreover, in cases such as double-layered reinforcement, shadowed areas may appear, making analysis difficult.

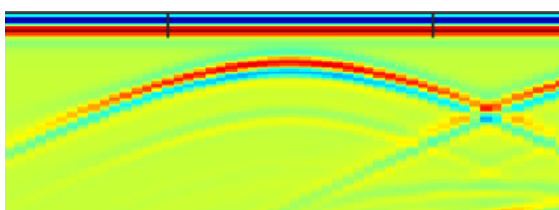


Figure 1. Hyperbola seen in a B-scan when rebar is present in concrete

To compensate for these shortcomings of image focusing methods, this study aims to develop an algorithm that determines the size of the rebar by analyzing the hyperbola seen in B-scan images—strictly speaking, this curve is not a perfect hyperbola but one that closely resembles it, and is commonly referred to as such.

## 2 PROBLEM DEFINITION AND SOLUTION

### 2.1 Definition of “Hyperbola”

When rebar is present inside concrete, a B-scan taken on a plane parallel to the rebar’s cross-section shows a hyperbola, as in Figure 1. If it is assumed that the rebar has a perfectly circular cross-section and that the transmitting and receiving antennas are located at the same position (mono-static), the principle behind the formation of this hyperbola can be explained by Figure 2.

In Figure 2, the gray area represents concrete and the white area represents the rebar. The variables  $r_r$ ,  $T$  and  $\bar{T}$  correspond to the rebar radius, the distance from the transmitter/receiver antenna to the surface of the rebar, and the rebar-related information actually recorded by the transmitter/receiver antenna in the B-scan, respectively.

Because the transmitter/receiver antenna transmits electromagnetic waves in all directions and receives waves from all directions, it only knows the time difference between transmission and reception; it does not know which direction the wave traveled. At each position of the antenna, the signal strength is recorded over time and plotted with the vertical axis as time (or distance) and the horizontal axis as the antenna’s location. By displaying signal intensity as color, one obtains a B-scan similar to Figure 1. Conventionally, the time axis in a

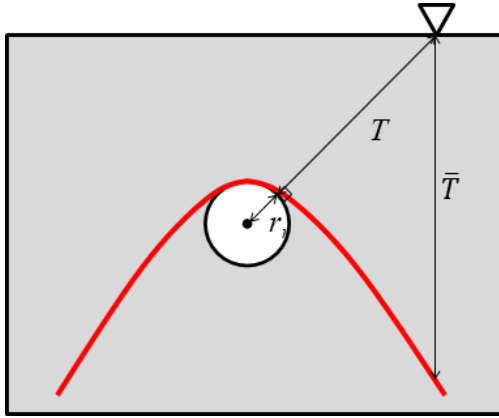


Figure 2. Principle behind hyperbola formation in the B-scan when rebar is present in concrete

B-scan represents half the round-trip time of the wave, effectively the one-way travel time. When the dielectric constant is known and assumed constant, this time can easily be converted into distance. For simplicity, the discussion here assumes the vertical axis represents the one-way travel distance of the electromagnetic wave.

In Figure 1, a hyperbola commonly appears in the B-scan. This hyperbola can be idealized by the red curve in Figure 2. For instance, when the transmitter/receiver antenna is located at the inverted triangle in Figure 2, the electromagnetic wave emitted by the transmitter reflects off the rebar and then returns to the receiver. Because the angle of reflection equals the angle of incidence, only the wave that follows the normal vector of the (assumed circular) rebar cross-section can return to the receiver. Therefore, the wave travels a distance of  $T$  to reach the rebar, reflects, and then travels the same distance  $T$  to reach the receiver. In the B-scan (Figure 1), the reflected signal from the rebar appears at a vertical distance of  $T$  beneath the antenna's position. If this vertical distance is denoted by  $\bar{T}$ , then in an ideal situation with no external interference and no measurement error,  $\bar{T}$  should be equal to  $T$ . The term  $T$  is the distance from the rebar center to the antenna minus the rebar radius; using Figure 3, it can be expressed as follows:

$$T(x, r_x, r_y, r_r) = \sqrt{(r_x - x)^2 + r_y^2} - r_r \quad (1)$$

Here,  $x$ ,  $r_x$ , and  $r_y$  denote the antenna's horizontal position, the rebar center's horizontal coordinate, and its vertical

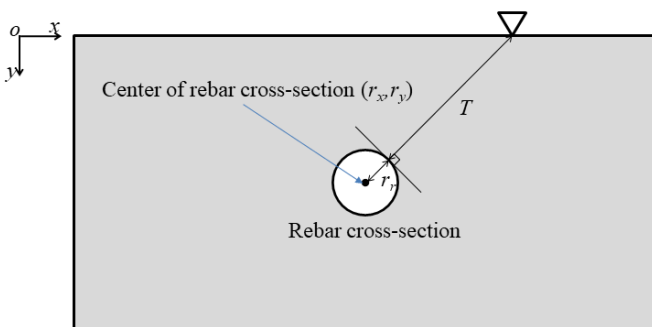


Figure 3. Travel distance of the electromagnetic wave upon reflection

coordinate, respectively. In Equation (1), if the rebar radius  $r_r$  is set to zero—in other words, if the cross-section of the material embedded in the concrete is assumed to be a point—the curve becomes a perfect hyperbola. It is for this reason that the curves in Figures 1 and 2 are commonly referred to as “hyperbolas.”

## 2.2 Estimation of the Rebar Radius in the Form of an Inverse Analysis

As explained above, in an ideal situation without any measurement error,  $T = \bar{T}$  holds in Figure 2. By substituting three pairs of  $(x, \bar{T})$  into Equation (1) and solve the simultaneous equations, the rebar radius  $r_r$  can be found. However, because actual measurements are subject to various errors, the measured  $\bar{T}$  inevitably includes some error. As a result, the value of  $r_r$  obtained using only three pairs of  $(x, \bar{T})$  can be extremely sensitive to even slight errors.

To reduce such errors, Multiple  $(x, \bar{T})$  pairs is used to solve an inverse problem defined by the following optimization equation:

$$\min_{r_x, r_y, r_r} \frac{1}{2} \int_A \|\bar{T} - T(x, r_x, r_y, r_r)\|_2^2 dx \quad (2)$$

In this equation, the integration domain  $A$  covers all  $x$  values where measurements were made. Discretizing this integral yield:

$$\min_{r_x, r_y, r_r} \frac{1}{2} \sum_{\text{for all } n} (\bar{T}_n - T(x_n, r_x, r_y, r_r))^2 \quad (3)$$

$\bar{T}_n$  and  $x_n$  denote the  $n$ -th measured  $(x, \bar{T})$  pair. Although Equations (2) or (3) can be solved by various methods, because the gradient vector and the Hessian matrix can be derived analytically, Newton's method provides an efficient way to obtain a solution.

## 3 NUMERICAL EXAMPLE

### 3.1 General Rebar Example

To analyze the error sensitivity of the proposed method, a numerical example was employed to verify Equation (3). In general, non-destructive testing equipment that uses electromagnetic waves discretizes the signals received by the receiver antenna. As shown in Figure 1, because only discrete points on the hyperbola can be recorded, the actual measurement cannot produce a smooth curve; instead, it is represented by quantized (or gridded) points. Such quantization becomes a significant source of error when using Equation (1) to fit to the measurement points for solving Equation (3). Various other errors that inevitably occur during the measurement process also contribute substantially to the instability of Equation (3).

To verify the stability against these errors, a numerical example was created using Equation (1), and then Equation (3) was solved using Newton's method to obtain a solution. The details of the example are as follows:

- Rebar radius: 12 mm

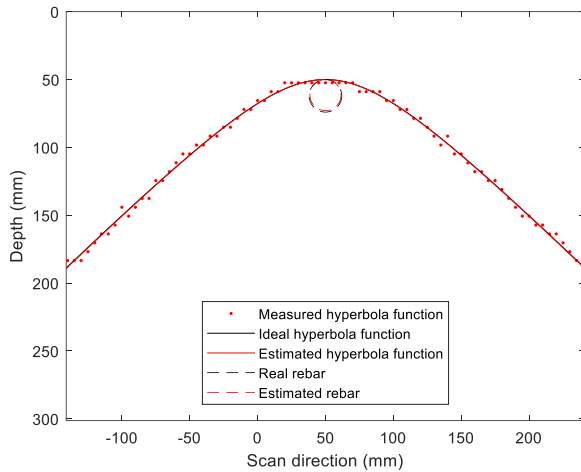


Figure 4. General rebar example and the resulting estimation of the rebar radius

- Concrete cover: 50 mm
- Rebar spacing: 50 mm
- Spatial sampling frequency: once per 5 mm
- Time sampling frequency: 20.48 GHz
- Relative permittivity of concrete: 5

It was assumed that the measuring device is Proceq's GP8800 [6]. The horizontal axis was discretized based on the number of scans per unit distance, and the vertical axis was discretized based on the temporal sampling rate and the relative permittivity. Up to 3% uniformly distributed white noise was added to the hyperbola generated by Equation (1), and the data were placed at the nearest discretized (grid) point.

Figure 4 shows the results of this example. The black dashed line indicates the actual rebar cross-section, and the black solid line represents the hyperbola derived from Equation (1). After adding white noise and mapping it onto the discretized grid, the red points appear in a stepwise manner rather than forming a smooth curve. It can also be observed that some points are distributed discontinuously because of the white noise.

Using the  $(x, \bar{T})$  pairs of these red points to solve Equation (3), the rebar radius was estimated to be 12.229 mm. The rebar radius and center location obtained from the estimation are plotted as a red dashed line in Figure 4, showing a good match with the actual location and radius.

### 3.2 Double-Layered Rebar Example

When the rebar is double-layered, as shown in Figure 5, information about the rebar behind the front one is obscured. Figure 5(a) shows the B-scan image, and Figure 5(b) illustrates a schematic representation. The obscured region is where the curve undergoes the most significant change, and thus contains the greatest amount of information. If a typical image-focusing post-processing method is applied to this image, almost no meaningful information about the rebar can be extracted. However, by employing the proposed inverse hyperbola analysis method, the rebar radius can still be estimated in such cases. The same conditions as the previous example were used, with the concrete cover doubled and a shadow region created extending five times the rebar radius from its center. As shown

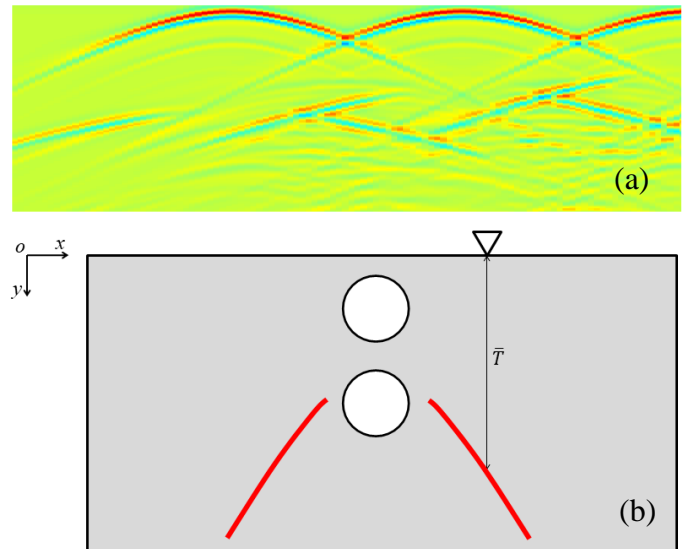


Figure 5. Double-layered rebar as seen via B-scan: (a) B-scan and (b) Schematic

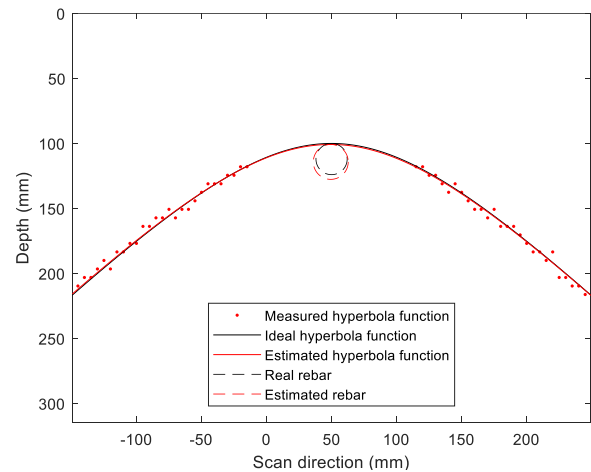


Figure 6. Simulation example of double-layered rebar and the resulting rebar radius estimation

in Figure 6, this setup is similar to the previous example but lacks measurement points near the rebar. By solving Equation (3), the rebar radius was estimated to be 13.42 mm. Although the accuracy is lower compared to the earlier example, it still represents a reasonably good estimation of the rebar radius

## 4 CONCLUSION

- An inverse-analysis-based method for estimating the rebar radius is proposed, which utilizes the hyperbolas observed in B-scans. By treating the rebar center coordinates and radius as unknown variables and formulating an optimization problem that minimizes the least-squares error, it becomes possible to determine the precise size of rebar cross sections—information that is difficult to obtain using conventional image-focusing techniques.
- The proposed rebar radius estimation method was verified through numerical examples. In a scenario with a typical rebar arrangement, the method accurately estimated the

rebar radius. It also performed well for the multi-layered rebar

- By presenting an inverse analysis approach for explicitly estimating the rebar radius, the proposed method overcomes limitations of existing non-destructive testing techniques. It can be effectively applied to detailed analyses of internal concrete structures. With ongoing research to refine  $(x, \bar{T})$  pair extraction and address numerical instabilities, even higher levels of accuracy can be expected in the future.

## ACKNOWLEDGMENTS

This research was funded by the Korea Institute of Civil Engineering and Building Technology (KICT) of the Republic of Korea, Project No. 2025-0057 (Concrete CT: Reinforcement Damage).

## REFERENCES

- [1] C. Özdemir, Ş. Demirci, E. Yiğit, and B. Yilmaz, A Review on Migration Methods in B-scan Ground Penetrating Radar Imaging. *Mathematical Problems in Engineering*, 2014.
- [2] J. Gazdag, Wave Equation Migration with the Phase-Shift Method. *Geophysics*, 43(7), 1978, 1342–1351.
- [3] Q. Yao and W. Qifu, Kirchhoff Migration Algorithm for Ground Penetrating Radar Data. In 2012 International Conference on Computer Science and Electronics Engineering (ICCSEE), vol. 2, IEEE, 2012, 396–398.
- [4] K. Dinh, T. T. Pham, T. T. Nguyen, and H. H. Vu, Application of Synthetic Aperture Focusing Technique to Visualize GPR Data from Reinforced Concrete Structures. *IOP Conference Series: Materials Science and Engineering*, 869(5), IOP Publishing, 2020, p. 052072.
- [5] H. Choi, J. Bittner, and J. S. Popovics, Comparison of Ultrasonic Imaging Techniques for Full-Scale Reinforced Concrete. *Transportation Research Record*, 2592(1), 2016, 126–135.
- [6] Proceq, Proceq GPR GP8000/GP8100/GP8800 User Manual (Version 1.0), Proceq SA, Schwerzenbach, Switzerland, 2024.